

## Pseudo-intramolecular behaviour of near-edge X-ray absorption fine structure from an atomic adsorbate

This article has been downloaded from IOPscience. Please scroll down to see the full text article.

1991 J. Phys.: Condens. Matter 3 7751

(<http://iopscience.iop.org/0953-8984/3/39/020>)

View [the table of contents for this issue](#), or go to the [journal homepage](#) for more

Download details:

IP Address: 171.66.16.96

The article was downloaded on 10/05/2010 at 19:59

Please note that [terms and conditions apply](#).

## LETTER TO THE EDITOR

# Pseudo-intramolecular behaviour of near-edge x-ray absorption fine structure from an atomic adsorbate

D Purdie†, C A Muryn†, N S Prakash†§, K G Purcell†, P L Wincott†, G Thornton† and D S-L Law‡

† Interdisciplinary Research Centre in Surface Science and Chemistry Department, Manchester University, Manchester M13 9PL, UK

‡ SERC Daresbury Laboratory, Warrington WA4 4AD, UK

Received 24 July 1991

**Abstract.** The polarization dependence of the Cl K-edge ‘white-line’ has been measured from Si(111)7 × 7-Cl and Si(100)2 × 1-Cl. In both cases it has the form expected on the basis of a pseudo-intramolecular  $\sigma^*$ -resonance model. This suggests that the near-edge x-ray absorption fine structure (NEXAFS) could provide a simple, incisive monitor of the surface structure for atomic adsorbates on semiconductors. Together with the corresponding surface extended x-ray absorption fine structure (SEXAFS), the Si(100)2 × 1-Cl NEXAFS indicates that Cl bonds atop a buckled dimer with a Cl-Si bond length of  $2.00 \pm 0.02$  Å.

Pioneering work by Stöhr *et al* [1] demonstrated that the near-edge x-ray absorption fine structure (NEXAFS) of molecular adsorbates is dominated by resonances within the adsorbed molecule. The energy and polarization dependence of these resonances can provide a simple measure of the adsorbate bond length and orientation [1, 2]. In sharp contrast, the NEXAFS from atomic adsorbates on metal substrates is thought to be dominated by long-range multiple scattering [3]. Modelling the spectra then requires computationally intensive multiple scattering calculations. In recent work we presented calculations for Cl adsorbed on Si surfaces which suggest that for atomic adsorbates on semiconductors the NEXAFS may display pseudo-intramolecular behaviour [4]; this difference would arise from the more local nature of adsorbate–semiconductor bonding. This being the case, NEXAFS could be used to provide an indication of the adsorbate–substrate bond length and geometry in the same manner as it is employed for molecular adsorbates.

In this work we have tested these ideas by measuring the polarization dependence of the Cl 1s  $\rightarrow \sigma^*$  bound-state resonance feature present in the Cl K-edge NEXAFS of Si(111)7 × 7-Cl and Si(100)2 × 1-Cl [4]. The results confirm the pseudo-intramolecular nature of the  $\sigma^*$  resonance, and we use this to determine the Si–Cl bond orientation on Si(100)2 × 1. Contrary to the conclusions of previous work, which employed electron energy loss spectroscopy [5], the Si–Cl bond is found to lie along the surface normal. In

§ Present address: Department Chemie Appliquée et Genie Chimique, CNRS UA417, 43 Boulevard du 11 Novembre 1918, F-69622 Villeurbanne Cédex, France.

conjunction with surface extended x-ray absorption fine structure (SEXAFS) measurements, the data indicate that Cl bonds atop a buckled dimer.

Chlorine K-edge NEXAFS and SEXAFS measurements were carried out using a Ge(111) crystal pair in the double-crystal monochromator of station 6.3 [6] at the SRS, Daresbury Laboratory. A double-pass cylindrical mirror analyser (CMA) (Physical Electronics Inc.) operated in the non-retard mode was used to record the Cl KLL Auger yield ( $E_k = 2370$  eV) as a monitor of the surface absorption coefficient. At the Cl K-edge (2824 eV) the x-ray beam is close to 100% plane polarized. The CMA axis was at  $90^\circ$  to the incident photon beam. Normalization of the Auger yield data to incident x-ray flux was accomplished using the electron yield from a thin beryllium foil placed between the monochromator and the sample chamber. NEXAFS were recorded at  $5^\circ$  intervals in the angle of incidence range  $5^\circ \leq \theta \leq 90^\circ$ , with the x-ray  $E$ -vector in the  $[\bar{1}10]$  azimuth of the Si(111) surface. For Si(100) $2 \times 1$ -Cl, two azimuthal geometries were employed; one in which the x-ray  $E$ -vector was in the  $[01\bar{1}]$  azimuth the other having the  $E$ -vector in the  $[011]$  azimuth. Measurements were carried out with the sample at room temperature ( $\sim 293$  K) and at a base pressure of  $< 1 \times 10^{-10}$  mbar.

Si wafer samples were used, with vicinal Si(100) wafers cut  $4^\circ$  off the (100) plane towards  $[011]$  used to obtain single domain surfaces [7]. Samples were cleaned *in situ* by resistive heating up to  $\sim 1100$  K, resulting in surface contamination below the level of detection by Auger electron spectroscopy (AES). The low energy electron diffraction (LEED) patterns obtained indicated the presence of well-ordered Si(111) $7 \times 7$  and single-domain ( $> 90\%$ ) Si(100) $2 \times 1$  surfaces. The clean surface was exposed to chlorine by dissociating AgCl in an electrochemical cell [8], the sample being maintained at  $\sim 500$  K during exposure to ensure that weakly bound chloride phases were not formed on the surface [9, 10]. The clean surface LEED patterns were retained after chlorine exposure with the appearance of additional intensity of the Si(100) $2 \times 1$   $[011]$ -direction half-order beams.

SEXAFS data were analysed using EXCURV90, a modelling routine based on the rapid curved wave computational scheme [11]. Phase shifts and backscattering amplitudes were obtained from SiCl<sub>4</sub> Cl K-edge EXAFS, in which the Si-Cl bond distance is  $2.018 \pm 0.003$  Å [12]. For Si(111) $7 \times 7$ -Cl, our SEXAFS results indicate an atop Cl geometry with a Cl-Si bond distance of  $2.00 \pm 0.02$  Å. This is consistent with earlier SEXAFS work on this surface, which determined that Cl sits atop Si adatoms of the  $7 \times 7$  reconstructed surface [13].

Figure 1 shows Cl K-edge NEXAFS spectra of Si(111) $7 \times 7$ -Cl after normalization to the absorption-edge step. The white line at  $\sim 5$  eV above the absorption edge was assigned by Citrin *et al* [13] to a transition between Cl 1s and predominantly (Cl, Si) 3p-derived  $\sigma_z^*$  states, with higher-lying features arising from excitation into Cl  $\pi_{x,y}^*$  states. Our NEXAFS calculations suggest that the 1s  $\rightarrow \sigma^*$  resonance may display pseudo-intramolecular behaviour [4]. In figure 1 the intensity of this feature can be seen to increase in intensity towards grazing incidence where the x-ray  $E$ -vector is parallel to the Si-Cl bond. Following procedures used in studies of intra-molecular resonances [14], a background was obtained from the normal incidence data by fitting the edge to an arctan function. This was subtracted from the spectra to partly isolate the  $\sigma^*$  resonance. An alternative method, involving subtraction of the normal incidence spectrum [14] was also employed. Although the two methods give essentially the same result, we use the results obtained from the latter method since it is free from fitting parameters. The background subtracted peaks are of a symmetric Gaussian form and this function was fitted to the resonance to isolate it from overlapping higher-energy features. The fitted

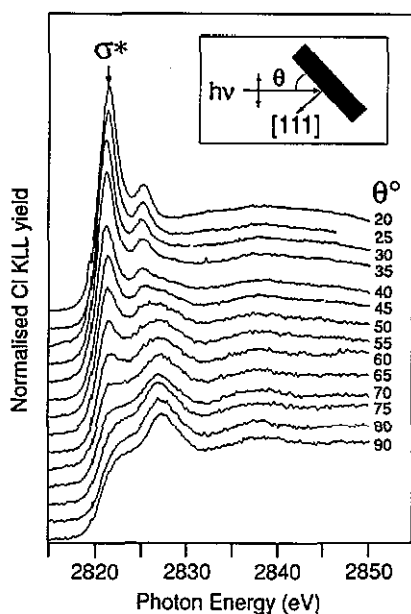


**Figure 1.** Cl K-edge Cl KLL Auger yield NEXAFS for Si(111)7  $\times$  7-Cl as a function of x-ray incidence angle,  $\theta$ . The pseudo-intramolecular  $\sigma^*$  resonance is indicated.

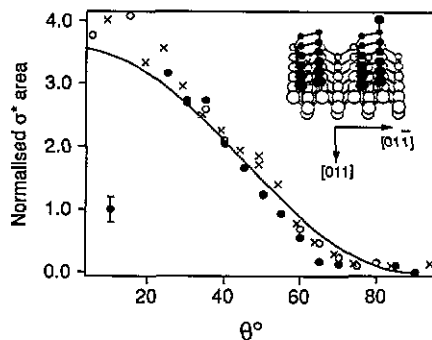


**Figure 2.** The edge-step-normalized Gaussian area of the Cl K-edge  $\sigma^*$  resonance from Si(111)7  $\times$  7-Cl (full circles) and Si(100)2  $\times$  1-Cl ([011] azimuth, crosses; [01 $\bar{1}$ ] azimuth, open circles). The full curve shows the result of a least squares fit of the Si(111)7  $\times$  7-Cl data to the function  $A \cos^2 \theta$ . The inset shows the proposed bonding site for Cl on the upper Si atom of a Si(100)2  $\times$  1 buckled dimer.

peaks have a constant ( $2.0 \pm 0.2$  eV) FWHM (full width half maximum), as expected for a pseudo-intramolecular resonance. Figure 2 shows the edge-step-normalized Gaussian area of the  $\sigma^*$  resonance plotted as a function of photon incidence angle for the Si(111)7  $\times$  7-Cl surface. The  $\cos^2 \theta$  polarization dependence is that expected for a Si-Cl-localized  $\sigma^*$  resonance, representing a dipole transition from an initial s state to a final state with  $\sigma$  symmetry [1]. This clearly supports the conjecture that the  $\sigma^*$  resonance is pseudo-intramolecular in nature. Although the higher energy structure in the NEXAFS appears to have a related intensity dependence, our calculations [4] suggest that this region of the spectrum is complicated by the presence of long-range multiple scattering effects.

The Si(100)2  $\times$  1-Cl Cl K-edge NEXAFS data are essentially the same as those of Si(111)7  $\times$  7-Cl, with the white line appearing at the same energy,  $\sim 5$  eV above the absorption edge. These observations provide further grounds to support the proposition that the NEXAFS data are dominated by short-range-scattering and that the resonance has pseudo-intramolecular character. By analogy with molecular adsorbate NEXAFS [2], the position of the  $\sigma^*$  resonance indicates that the Cl-Si bond length on Si(111)7  $\times$  7-Cl is close to that on Si(100)2  $\times$  1-Cl. This is confirmed by our SEXAFS data (see below).

The polarization dependence of molecular resonances in NEXAFS has proved to be a powerful technique for determining the orientation of molecules on surfaces [15]. Here

we explore the use of polarization-dependent measurements of the Si-Cl  $\sigma^*$  resonance to determine the Si-Cl bond geometry on Si(100) $2 \times 1$ -Cl. An electron energy loss study concluded that Cl adsorbs at step or defect sites on Si(100) $2 \times 1$  [5]. However, others have supposed that Cl atoms saturate the dangling bonds on both atoms of each dimer resulting in a symmetric dimer structure [7]. This would be consistent with recent angle-resolved photoemission work on Cl and monohydride terminated Si(100) $2 \times 1$  [7]. Scanning tunnelling microscopy (STM) results for the monohydride phase also show the presence of H atoms at both ends of surface dimers [16]. With symmetric dimers, the tetrahedral angle places the Si-Cl bond in the dimer plane, inclined at  $19^\circ$  to [100]. On the vicinal surfaces employed here, the Si dimer bonds are oriented parallel to  $[01\bar{1}]$ .

On the basis of a symmetric dimer model, the NEXAFS in the  $[011]$  and  $[01\bar{1}]$  azimuths should be noticeably different. In the  $[011]$  azimuth, where the x-ray  $E$ -vector is perpendicular to the dimer plane, the white line should have zero intensity at normal incidence, increasing towards grazing incidence. Data in the  $[01\bar{1}]$  azimuth, which contains the dimer bond, should show a finite intensity at normal emission increasing towards the same limit as the  $[011]$ -azimuth data at grazing incidence. However, a comparison of the edge-step-normalized normal incidence spectra in the two azimuths reveals very little difference. Moreover, the polarization dependence in both azimuths is essentially the same as that seen in figure 1 for Si(111) $7 \times 7$ -Cl. Subtracting the normal incidence spectrum recorded in the  $[011]$  azimuth from the data in the same manner as that employed for the Si(111) $7 \times 7$ -Cl data, yields the variation in the edge-step-normalized Gaussian area of the  $\sigma^*$  resonance shown in figure 2. A comparison of the data in figure 2 confirms that the resonance behaviour in both azimuths of Si(100) is the same as that observed from Si(111) $7 \times 7$ -Cl. This similarity extends to the three data sets having comparable edge-step-normalized peak areas at all angles of x-ray incidence. Hence, the NEXAFS results indicate that the Si-Cl bond is perpendicular to the (100) surface to within  $10^\circ$ .

To examine this unexpected result further, we turn to the SEXAFS data. No discernable EXAFS are present in data recorded at normal incidence with the  $E$ -vector in either azimuth. Hence spectra resemble the normal-incidence SEXAFS spectra of Si(111) $7 \times 7$ -Cl [13], indicating a Si-Cl bond lying within  $10^\circ$  of [100]. The grazing incidence SEXAFS data from separately prepared samples in both azimuths give a Cl-Si bond distance of  $2.00 \pm 0.02 \text{ \AA}$ , identical to that determined for Si(111) $7 \times 7$ -Cl. The superior quality of the present data leads to a better estimate of the bond distance than that previously reported for the (100) surface,  $1.95 \pm 0.04 \text{ \AA}$  [4].

Additional information about the surface structure is gained by considering the Cl backscattering contribution to the Cl K-edge SEXAFS. A Si(100) $2 \times 1$  surface unit cell has dimensions  $3.84 \text{ \AA}$  in the  $[011]$  direction and  $7.68 \text{ \AA}$  in the  $[01\bar{1}]$  direction and calculations predict that the Si-Si distance within a dimer is about that of the bulk Si bond distance,  $2.35 \text{ \AA}$  [17]. If Cl atoms occupy both Si dimer sites in an atop geometry, consistent with the NEXAFS, then strong Cl backscattering would be observed in the normal-incidence SEXAFS when the  $E$ -vector was parallel to the dimer. This amplitude is still large in this experimental geometry if the Si-Cl bonds are angled away from each other along the dimer axis. In this case Cl backscattering would be observed from Cl atoms occupying adjacent dimers along  $[01\bar{1}]$ . For instance, with a Si-Cl bond angle of  $20^\circ$  to [100] the inter-dimer Cl-Cl distance is  $3.84 \text{ \AA}$ , equal to the intra-dimer Cl-Cl distance. That no Cl-Cl backscattering contribution is observed in the normal incidence SEXAFS indicates that the Cl coverage is much less than has previously been assumed

[7]. The relative Cl K edge-jumps of Si(111)7 × 7-Cl and Si(100)2 × 1-Cl and the corresponding AES Cl LMM/Si LMM peak ratios are consistent with this observation. These are the similar on both surfaces, the AES peak ratios being  $0.50 \pm 0.15$ , and the edge jumps being  $40 \pm 5\%$  at grazing photon incidence and  $70 \pm 5\%$  at normal incidence in each case. The average area per adatom site is  $52 \text{ \AA}^2$  on Si(111)7 × 7 and on the Si(100)2 × 1 surface each surface unit cell of area  $30 \text{ \AA}^2$  contains one dimer. A simple comparison of the edge jumps and areas, which assumes that all adatom sites are occupied on Si(111)7 × 7, indicates a coverage of between one and  $\frac{1}{2}$  Cl atoms per dimer on Si(100)2 × 1.

A geometry in which the Si-Cl bond is perpendicular to the (100) surface suggests that Cl sites atop a buckled (asymmetric) dimer. This would result in a local geometry of Cl similar to that of the adatoms of the (111)7 × 7 surface, explaining the close similarity of the Cl K-edge NEXAFS and angle-resolved photoemission data recorded at normal emission [7, 10]. A random distribution of Cl on such sites, with less than one Cl atom per dimer (see figure 2) would be consistent with the absence of a noticeable Cl backscattering in the SEXAFS. That the LEED pattern formed on adsorption displays enhanced intensity in the positions of the extra half order beams indicates a degree of etching by Cl, stripping away the top layer Si atoms. Such etching by Cl has been observed for Si(111)7 × 7 [18] and H-induced etching of Si(100)2 × 1 has been demonstrated [16].

This work suggests that NEXAFS from atomic adsorbates on semiconductors could provide the same simple, incisive probe of the bond geometry currently employed for molecular adsorbates. A particularly promising area of application lies in the study of intermediates associated with etching and oxidation processes.

This work was funded by the United Kingdom Science and Engineering Research Council. Additional support was provided by Johnson Matthey plc.

## References

- [1] Stöhr J and Jaeger R 1982 *Phys. Rev. B* **26** 4111
- [2] Sette F, Stöhr J and Hitchcock A P 1984 *J. Chem. Phys.* **81** 4906
- [3] See for example,  
Norman D, Stöhr J, Jaeger R, Durham P J and Pendry J B 1983 *Phys. Rev. Lett.* **51** 2052
- [4] Thornton G, Wincott P L, McGrath R, McGovern I T, Quinn F M, Norman D and Vvedensky D D 1989 *Surf. Sci.* **211/212** 959  
Purdie D, Murny C A, Prakash N S, Wincott P L, Thornton G and Law D S-L 1991 *X-ray Absorption Fine Structure* (ed) S Hasnain (Chichester: Ellis Horwood) p 209
- [5] Aoto N, Ikawa E and Kurogi Y 1988 *Surf. Sci.* **199** 408
- [6] MacDowell A A, Norman D and West J B 1986 *Rev. Sci. Instr.* **57** 2667
- [7] Johansson L S O, Uhrberg R I G, Lindsay R, Wincott P L and Thornton G 1990 *Phys. Rev. B* **42** 9534
- [8] Spencer N D, Goddard P J, Davies P W, Kitson M and Lambert R M 1983 *J. Vac. Sci. Technol. A* **1** 1554
- [9] Jackman R B, Ebert H and Foord J S 1986 *Surf. Sci.* **176** 183
- [10] Schnell R D, Rieger D, Bogen A, Himpfel F J, Wandelt K and Steinmann W 1985 *Phys. Rev. B* **32** 8057
- [11] Gurman S J, Binstead N and Ross I 1984 *J. Phys. C: Solid State Phys.* **17** 143
- [12] Ryan R R and Hedberg K 1969 *J. Chem. Phys.* **50** 4986
- [13] Citrin P H, Rowe J E and Eisenberger P 1983 *Phys. Rev. B* **28** 2299
- [14] Outka D A and Stöhr J 1988 *J. Chem. Phys.* **88** 3539
- [15] Stöhr J and Outka D A 1987 *Phys. Rev. B* **36** 7891
- [16] Boland J J 1990 *Phys. Rev. Lett.* **65** 3325
- [17] see for example, Batra I P 1990 *Phys. Rev. B* **41** 5048
- [18] Boland J J and Villarrubia J S 1990 *Phys. Rev. B* **41** 9865